



This is a repository copy of *High mobility In_{0.75}Ga_{0.25}As quantum wells in an InAs phonon lattice*.

White Rose Research Online URL for this paper:
<http://eprints.whiterose.ac.uk/128422/>

Version: Accepted Version

Article:

Chen, C., Holmes, S.N., Farrer, I. orcid.org/0000-0002-3033-4306 et al. (2 more authors) (2018) High mobility In_{0.75}Ga_{0.25}As quantum wells in an InAs phonon lattice. *Journal of Physics: Condensed Matter*, 30 (10). 105705. ISSN 0953-8984

<https://doi.org/10.1088/1361-648X/aaa947>

This is an author-created, un-copyedited version of an article accepted for publication/published in *Journal of Physics: Condensed Matter*. IOP Publishing Ltd is not responsible for any errors or omissions in this version of the manuscript or any version derived from it. The Version of Record is available online at <https://doi.org/10.1088/1361-648X/aaa947>

Reuse

Items deposited in White Rose Research Online are protected by copyright, with all rights reserved unless indicated otherwise. They may be downloaded and/or printed for private study, or other acts as permitted by national copyright laws. The publisher or other rights holders may allow further reproduction and re-use of the full text version. This is indicated by the licence information on the White Rose Research Online record for the item.

Takedown

If you consider content in White Rose Research Online to be in breach of UK law, please notify us by emailing eprints@whiterose.ac.uk including the URL of the record and the reason for the withdrawal request.

High mobility $\text{In}_{0.75}\text{Ga}_{0.25}\text{As}$ quantum wells in an InAs phonon lattice

C. Chen

Cavendish Laboratory, University of Cambridge, J. J. Thomson Avenue, Cambridge, CB3 0HE, United Kingdom

E-mail: cc638@cam.ac.uk

S. N. Holmes

Toshiba Research Europe Limited, 208 Cambridge Science Park, Milton Road, Cambridge, CB4 0GZ, United Kingdom

E-mail: s.holmes@crl.toshiba.co.uk

I. Farrer*

Cavendish Laboratory, University of Cambridge, J. J. Thomson Avenue, Cambridge, CB3 0HE, United Kingdom

*Now at Department of Electronic and Electrical Engineering, The University of Sheffield, Mappin Street, Sheffield, S1 3JD, UK

E-mail: i.farrer@sheffield.ac.uk

H. E. Beere

Cavendish Laboratory, University of Cambridge, J. J. Thomson Avenue, Cambridge, CB3 0HE, United Kingdom

E-mail: heb1000@cam.ac.uk

D. A. Ritchie

Cavendish Laboratory, University of Cambridge, J. J. Thomson Avenue, Cambridge, CB3 0HE, United Kingdom

E-mail: dar11@cam.ac.uk

Abstract. InGaAs based devices are great complements to silicon for CMOS, as they provide an increased carrier saturation velocity, lower operating voltage and reduced power dissipation [1]. In this work we show that $\text{In}_{0.75}\text{Ga}_{0.25}\text{As}$ quantum wells with a high mobility, 15 000 to 20 000 $\text{cm}^2/\text{V}\cdot\text{s}$ at ambient temperature, show an InAs-like phonon with an energy of 28.8 meV, frequency of 232 cm^{-1} that dominates the polar-optical mode scattering from ~ 70 K to 300 K. The optical phonon frequency is insensitive to the carrier density modulated with a surface gate or LED illumination. We model the electron scattering mechanisms as a function of temperature and identify mechanisms that limit the electron mobility in $\text{In}_{0.75}\text{Ga}_{0.25}\text{As}$ quantum wells. Background impurity scattering starts to dominate for temperatures < 100 K. In the

high mobility $\text{In}_{0.75}\text{Ga}_{0.25}\text{As}$ quantum well, GaAs-like phonons do not couple to the electron gas unlike the case of $\text{In}_{0.53}\text{Ga}_{0.47}\text{As}$ quantum wells.

1. Introduction

In the $\text{In}_x\text{Ga}_{1-x}\text{As}$ alloy, the optical phonons exhibit a two-mode behaviour: both GaAs-like and InAs-like phonons exist across the whole composition range [2]. This has been of extensive interest to many researchers [3–10] and it was found that the dominant phonon mode can be controlled by varying the layer structure and the electron density [8, 11]. However, reports of dominant InAs-like phonons remains scarce with some reporting a contribution of InAs-like phonons from the InAlAs alloy in the barrier. A study [2] investigated this behavior and showed that the oscillator strength of InAs-like phonons is decreased due to the coupling by ionic polarisation field and hence InAs-like phonons can be absent even in In-rich samples.

In this paper, we report the detection of InAs-like phonons in $\text{In}_{0.75}\text{Ga}_{0.25}\text{As}/\text{In}_{0.75}\text{Al}_{0.25}\text{As}$ quantum wells (QW) with magneto-phonon resonance (MPR) measurements, a useful method to investigate electron-optical phonon interactions in 2 dimensional electron gas (2DEG) systems of heterostructures [11] that can establish the dominant phonon mode. The optical phonon frequency is insensitive to the substrate material and the carrier density in the range studied. An electron scattering rate model, using the optical-phonon energy obtained from the MPR measurement, of 28.8 meV, shows good agreement with the experimental mobility data.

2. Methods

The 30 nm wide $\text{In}_{0.75}\text{Ga}_{0.25}\text{As}$ QW confined between $\text{In}_{0.75}\text{Al}_{0.25}\text{As}$ barriers, is grown by solid-source molecular beam epitaxy (MBE) with linear-graded $\text{In}_x\text{Al}_{1-x}\text{As}$ buffers. This work studied samples grown on both GaAs and InP substrates to explore the possible effect of substrate on phonon properties. Many previous MPR studies were based on InGaAs grown on InP substrates [3–10] as $\text{In}_{0.53}\text{Ga}_{0.47}\text{As}$ is lattice-matched to InP and requires a thinner grading layer to grow high indium composition alloy. A peak mobility of $4.3 \times 10^5 \text{ cm}^2/\text{V.s}$ was observed at 1.5 K at $3.7 \times 10^{11} \text{ cm}^{-2}$ before the on set of the 2nd subband on sample A and B [12]. The electron mobility at ambient temperature has been increased from $9.0 \times 10^3 \text{ cm}^2/\text{V.s}$ [7] to $1.5 \times 10^4 \text{ cm}^2/\text{V.s}$ in this work. A detailed layered structure can be found in the literature [12, 13] and the samples are summarised in table 1.

Oscillations in magnetoresistance (MR) occurs when the optical phonon energy E_{ph} is equal to the separation between an integral number of Landau levels, giving an increased scattering rate and a maximum in resistivity.

$$E_{ph} = \hbar\omega_{LO} = N\hbar eB_N/m^* \quad (1)$$

$$\omega_{LO} = 2\pi\nu_{LO}C \quad (2)$$

where N is the resonance index, B_N is the field of resistivity maximum, the product $NB_N = B_f$ is the characteristic fundamental field of the resonance, ν_{LO} is the wave number (frequency, cm^{-1}) and C is the speed of light, $m^* = 0.039m_0$ is the effective electron mass taken from [14] (measured at 3.57 T) where the InGaAs growth strategy, carrier density (n_{2d}) and electron mobility are similar to the wafers reported here. The correction to m^* for non-parabolicity and polaron effects [6] is calculated to be 3 and 5% for $N = 2$ and 3.

Table 1. Sample Specification

Sample	Substrate	MD ^a / m^{-3}	Illumination	Top Gate	$n_{2d}/\times 10^{11} \text{ cm}^{-2}$
A	GaAs	1.8×10^{23}	No	Yes	2.8/3.5 (0/0.5V)
B	GaAs	1.8×10^{23}	No	No	2.5
C	GaAs	2.3×10^{23}	Yes	No	4.8
D	InP	2.3×10^{23}	No	No	0.87

^a MD: modulation doping

Longitudinal resistance in a Hall Bar geometry was measured in magnetic field up to 8 T at different temperatures $T=1.5 - 300$ K. As the MPR oscillation amplitude is small compared to the background resistance, either a signal proportional to the magnetic field is subtracted (this work, ΔR_{xx}) or the second derivative of the signal is taken [6].

3. Results and discussions

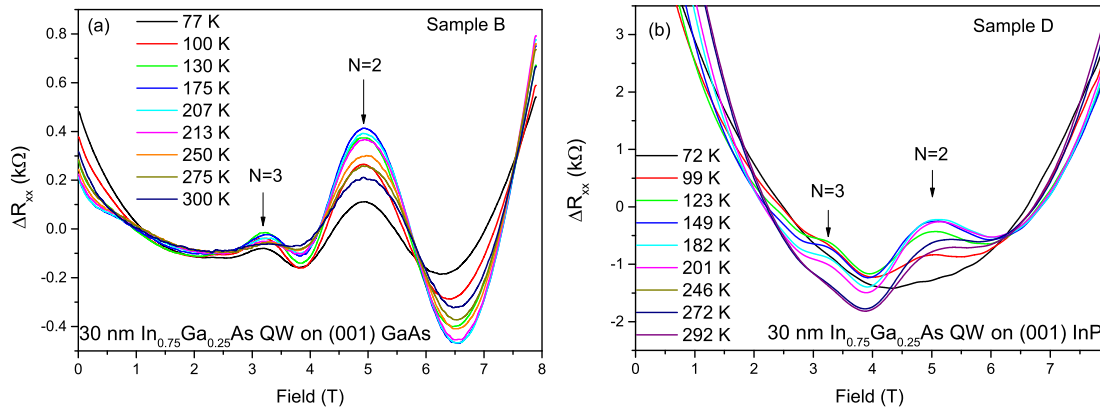


Figure 1. MR ($\Delta R_{xx} = \text{Longitudinal resistance} - \text{linear term}$) measured in InGaAs QWs grown on (001) GaAs substrate (a) and (001) InP substrate (b), displaying MPR up to room temperature. N with arrows depicts the resonance index.

At low temperatures, the Shubnikov-de Haas (SdH) oscillations dominate the MR but quickly dampen as the temperature increases. For temperatures higher than ~ 70 K, a series of oscillations developed due to MPR that can be observed up to 300

K. Representative results from two samples, shown in fig.1 (a) and (b), display well developed extrema at $N = 1\frac{1}{2}, 2, 2\frac{1}{2}, 3, 3\frac{1}{2}$.

With a linear background subtracted, the MR of both sample B and D show oscillations around similar magnetic field, demonstrating similar phonon energy. The difference between the MR of sample B and D is due to different conductivity between them because of more deep-level donor states accumulated across a thicker buffer in sample B. This has led to a lower measured 2D electron density in sample D, which is $8.7 \times 10^{10} \text{ cm}^{-2}$ at 1.5 K comparing with $2.5 \times 10^{11} \text{ cm}^{-2}$ in sample B, see table 1.

As seen in fig. 1, the oscillation amplitude increases with increasing temperature from above 70 K, reaching a maximum at ~ 175 K, and then gradually dropping as the temperature increases further. MPR can only be observed in a certain temperature range: at lower temperatures the LO phonon population drops, MPR due to the absorption of the LO phonons will no longer be observable and SdH becomes dominant in the MR [11] below 20 K; at high temperatures the oscillation amplitude is reduced by the thermal broadening of the Landau levels.

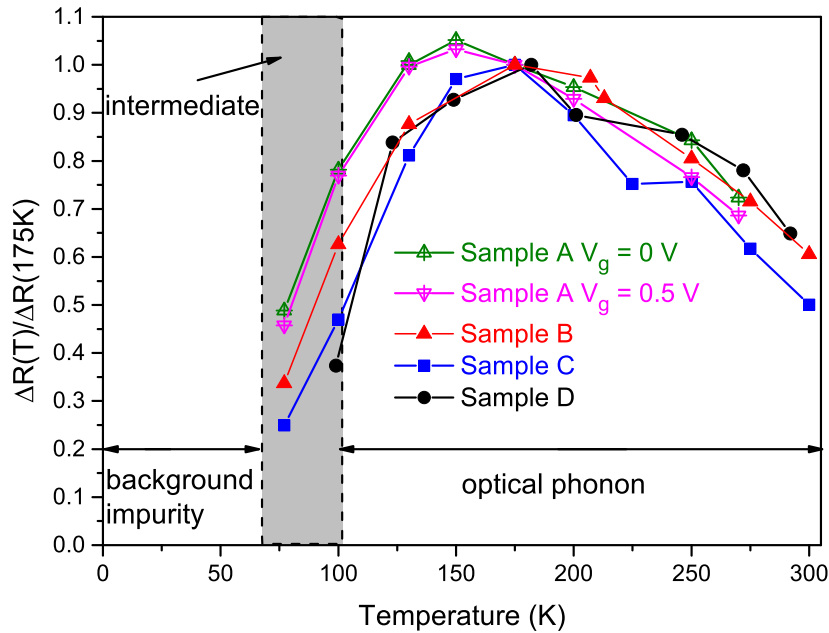


Figure 2. Relative MPR amplitude $\frac{\Delta R(T)}{\Delta R(175K)}$ as a function of temperature.

The relative amplitude ($\frac{\Delta R(T)}{\Delta R(175K)}$ between the extrema at $N = 2$ and 1.5) of the MPR is plotted in fig. 2. The relative amplitude maximum of sample A with a top gate has a slightly lower characteristic temperature than the others, around 150 K. This could be due to the SiO_2 insulator on top of the sample surface, modifying the interfacial optical mode at the InAlAs/ SiO_2 interface [15]. However for all the samples, the relative amplitude displays a maxima range from 150 K to 175 K. The relative amplitude falls off more rapidly when lowering the temperature than when raising it from the maxima range. This suggests that the effect of Landau level broadening on

MPR amplitude is weaker than that of the phonon depopulation, which demonstrates that the high crystalline quality in the samples and explains why the MPR is observable up to 300 K.

Within all these samples, only one phonon periodicity can be seen from the MPR oscillations. The resonance index is plotted versus the reciprocal of the magnetic field positions for the resistivity extrema in fig. 3. The gradient is the fundamental field B_f . All 4 samples show similar fundamental field, 9.6 - 9.8 T, as summarised in fig. 3. This is attributed to the dominant LO phonon with the energy (E_{ph} , calculated from equation 1) of 28.8 ± 0.3 meV at the frequency of 232 cm^{-1} which is the InAs-like LO phonon as only longitudinal phonons are active in carrier scattering [4]. This, however is not unexpected in terms of the oscillator strength.

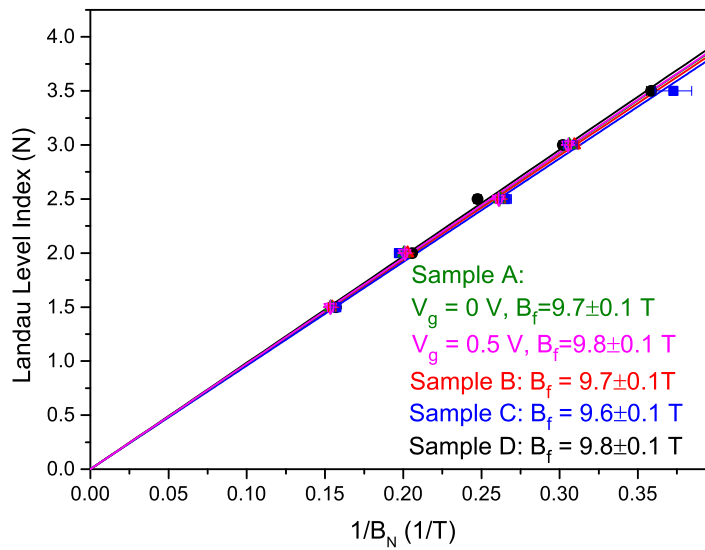


Figure 3. Resonance index N as a function of reciprocal extrema field position $\frac{1}{B_N}$ with $NB_N = B_f$, the fundamental field (the linear gradient).

The oscillator strength S is $\propto [\epsilon_0 - \epsilon']$ [5, 7], where ϵ_0 is low-frequency dielectric constants and ϵ' is defined by the generalised Lyddane-Sachs-Teller relations:

$$\frac{\epsilon_0}{\epsilon'} = \frac{\omega_L^2}{\omega_T^2} \quad (3)$$

where ω_L and ω_T are the LO and TO phonon frequencies.

Table 2. Possible Phonon Modes in InGaAs and InAlAs

	ϵ_0	ω_T (cm^{-1})	ω_L (cm^{-1})	$\omega_{T'}$ (cm^{-1})	$\omega_{L'}$ (cm^{-1})
$\text{In}_{0.75}\text{Ga}_{0.25}\text{As}$	14.4	224	235	248	259
$\text{In}_{0.75}\text{Al}_{0.25}\text{As}$	13.9	218	238	338	351

ω and ω' are for two different phonon modes in the ternary alloy, InAs and GaAs(AlAs) for InGaAs(InAlAs). The InAs phonon frequencies is highlighted blue.

The phonon modes in table 2 are extracted from the literature [16–18] and are for fully relaxed lattices. According to equation 3 and table 2, the oscillator strength of InAs-like phonon (blue) from $\text{In}_{0.75}\text{Ga}_{0.25}\text{As}$ ($[\epsilon_0 - \epsilon'] = 1.45$) is stronger than that of GaAs-like phonon in $\text{In}_{0.75}\text{Ga}_{0.25}\text{As}$ ($[\epsilon_0 - \epsilon'] = 1.31$). This result is in agreement with the literature [2]. Therefore, in $\text{In}_{0.75}\text{Ga}_{0.25}\text{As}$ quantum wells, InAs phonon oscillations are dominant in the MPR spectrum.

The optical-phonon behaviour is affected by three factors: the mass disorder, the microscopic strains and the coupling by the ionic polarisation field [2]. In this aspect, the samples presented in this work are different from what has already been reported. For InGaAs alloys, the latter two factors play more important roles in determining the oscillator strength and the coupling is more significant at high indium composition. For relaxed InGaAs with a lower In concentration, when the coupling is not so important, the microscopic strain built in the lattice due to local bond distortion is larger than that of the samples in this study, and therefore results in a smaller oscillator strength. In case of strained InGaAs with a similar In concentration and therefore the same amount of coupling, the compressive strain in the lattice also leads to a reduction of oscillator strength. This explains why GaAs dominant MPR have been reported in the literature.

Further measurement of magneto-resistance of sample B up to 13.25 T has been carried out to investigate the possibilities of peaks at higher field. $N = 1$ peak due to InAs-like phonon appeared at around 10.1 ± 0.3 T as seen in fig. 4. The data showed no additional peaks due to any phonons other than InAs-like. This is different from what is reported in Ref. [8] that AlAs-like phonon ($B_f = 19.2$ T) is seen at around 9 T.

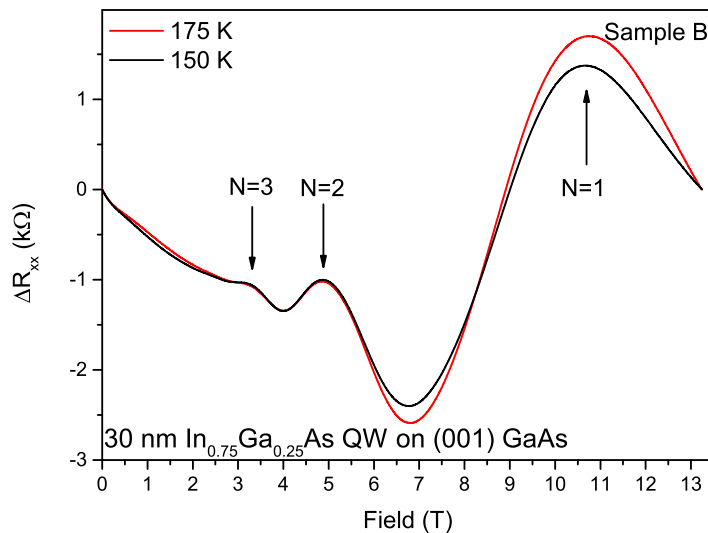


Figure 4. MR (ΔR_{xx} = Longitudinal resistance - linear term) measured in InGaAs QWs grown on (001) GaAs substrate, displaying MPR up to 13.25 T, showing a single frequency oscillation. N with arrows depicts the resonance index.

The fact that the InAs-like phonon is dominant in these samples is unlikely to be due to the contribution of InAs-like phonons in the InAlAs barrier as stated in the work based on InGaAs/InAlAs heterojunctions [7] since the QW width in this work is 30

nm, which is much wider than the previously studied system [6, 9]. There are three possible reasons why phonons from the barriers can play an important role in MPR: 1). wavefunction penetration, 2). remote scattering and 3). alloy scattering at the interface. It is not unreasonable to assume here that the wave function penetration (of the order of a few percent to the most) into the barrier is negligible providing that the MPR was measured at a relatively low carrier density. A simulated band profile of a similar structure with similar mobility is reported in [19], showing that the wave function is well contained in the QW with a single subband. Only with a good confinement, can we observe a high electron mobility of the order of $10^5 \text{ cm}^2\text{V}^{-1}\text{s}^{-1}$. Therefore, despite the InAs-like phonons in InAlAs having a larger oscillator strength than in InGaAs, the electron-phonon interaction in the well should contribute much more than that from the barrier due to the significantly reduced electron density. In discussing remote phonons from the barriers, reference [8] claims that the strength depends on the interfacial layer thickness and the wavefunction penetration. Given that we have a sharp interface [20] and small wavefunction penetration, we believe that the influence of the remote phonons, eg. InAs-like from $\text{In}_{0.75}\text{Al}_{0.25}\text{As}$, is negligible.

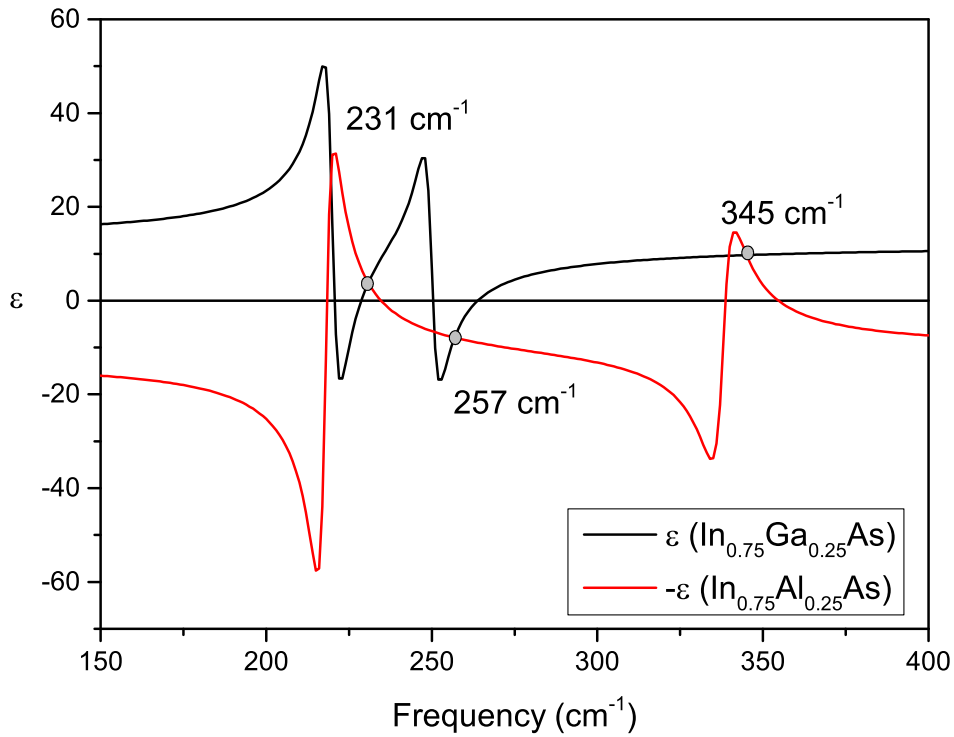


Figure 5. The plot of dielectric constants of $\text{In}_{0.75}\text{Ga}_{0.25}\text{As}$ and $\text{In}_{0.75}\text{Al}_{0.25}\text{As}$. The interface modes are found at the frequencies where $\epsilon_{\text{InGaAs}} = \epsilon_{\text{InAlAs}}$.

However, it is difficult to explicitly neglect the contributions from InAs-like phonons in the InAlAs barrier and at the interface. This is because that the InAs-like modes in the InGaAs well and the InAlAs barrier are both degenerate with the interface phonons. The possible LO interface phonon modes, estimated from the intersection points of the dielectric constant curves of $\text{In}_{0.75}\text{Ga}_{0.25}\text{As}$ and $\text{In}_{0.75}\text{Al}_{0.25}\text{As}$ [5, 17, 18], are 231, 257 and

345 cm^{-1} , see fig. 5, while the calculated values for InAs-like phonon in fully relaxed $\text{In}_{0.75}\text{Ga}_{0.25}\text{As}$ [18] and $\text{In}_{0.75}\text{Al}_{0.25}\text{As}$ [17] are 234 and 238 cm^{-1} respectively.

The periodicity of the MPR in this work shows no dependence on the carrier density. Sample A, measured at two different top gate voltages (V_g), and therefore two different carrier densities (20% increase of carrier density at 1.5 K), displays similar fundamental fields, $9.7 \pm 0.1 \text{ T}$ and $9.8 \pm 0.1 \text{ T}$ and therefore similar phonon energy 28.8 ± 0.3 and $29.1 \pm 0.3 \text{ meV}$. This small difference in phonon energy 0.3 meV is within the experimental error. The carrier density is increased (double that of sample A at 1.5 K) by illuminating sample C, which also showed a similar fundamental field that gives E_{ph} of $28.5 \pm 0.3 \text{ meV}$, again demonstrating the insensitivity of MPR periodicity to carrier density in these samples. Sample B and D, grown on (001) GaAs and (001) InP substrate respectively, have different carrier densities but very similar fundamental fields, which links to E_{ph} of $28.8 \pm 0.3 \text{ meV}$ and $29.1 \pm 0.3 \text{ meV}$. The phonon mode in the QW showed no dependence on carrier density and on the substrate, demonstrating that GaAs and InP are both good candidates for epi-grown InGaAs using graded buffer layers. The phonon spectrum is determined by the epi-structures in the active region, eg. wells and barriers.

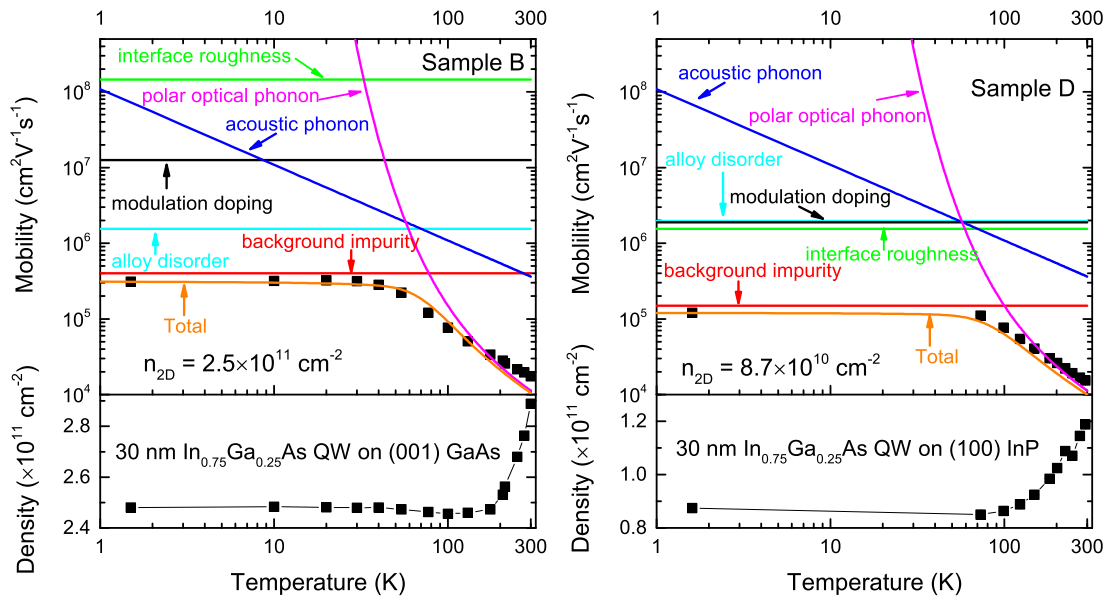


Figure 6. Comparison of temperature-dependent mobility simulation for 30 nm InGaAs QW using InAs-like optical phonons to measured density and mobility.

In contrast results on modulation doped $\text{In}_{0.53}\text{Ga}_{0.47}\text{As}/\text{InP}$ narrow wells [6] show that the phonon energy shifts from 33.7 meV to 28.4 meV with increasing carrier density. The behaviour of carrier density dependent optic phonon frequency was not yet fully understood at the time [6, 8]. One explanation is that the phonons couple to an intermediate mode, presented in the narrow well samples where $\omega_{01} > \omega_{LO}$, which decreases in frequency from the LO to the TO value as density increases. In wide QWs like this work, the inter-subband separation $\hbar\omega_{01} = 10.66 \text{ meV}$ is much less than the

phonon energy 28.8 meV, the intermediate phonon mode does not exist.

Temperature-dependent transport models have been developed on InGaAs QWs [21] and InGaAs heterostructures [22]. In this work, the scattering from background impurities is added as it is the dominant scattering mechanism at low carrier densities in In_{0.75}Ga_{0.25}As/In_{0.75}Al_{0.25}As QWs [12]. Scattering from acoustic phonon, polar optical phonon, background impurity, modulation doping, interface roughness and alloy disorder were considered here based on the work of Gold [23] and Price [24]. The parameters used for simulation are listed in table 3, whilst the simulation results for sample B on (001) GaAs substrate and sample D on (001) InP substrate are shown in fig. 6.

Table 3. Scattering Rate Simulation Parameters

Effective mass	m^*	$0.039m_e$ [14]
Deformation potential	D	9.4 eV [21]
Mass density of In _{0.75} Ga _{0.25} As	ρ	5580 kg/m ³
LA phonon velocity ([1 $\bar{1}$ 0])	μ_L	4527 m/s [16]
Optical phonon frequency	Ω_o	28.8 meV
Static dielectric constant	κ_0	$14.42\epsilon_0$
High frequency dielectric constant	κ_∞	$11.95\epsilon_0$
Alloy disorder potential	V_{AD}	0.3 eV [12]
Sample		B/D [12]
Intentional doping	N_{MD}	$2.3/1.8 \times 10^{23} \text{ m}^{-3}$
Unintentional doping	N_{BG}	$4.9/3.5 \times 10^{21} \text{ m}^{-3}$
Interface average height	Δ	3/6 Å
Interface correlation length	Λ	12/300 Å

The measured 2DEG carrier density used in the simulation is shown in fig. 6 for each sample. The carrier density increases at higher temperatures (> 200 K) and in this region, the scattering from optical phonons is dominant which is independent of the carrier density, therefore the effect of increased carrier density on the mobility is ignored during the simulation. The parameters that limit the low temperature mobility are first extracted from simulating mobility measured as a function of carrier density. Then the phonon energy measured from the experiment is applied to simulate the mobility change as a function of temperature. The scattering model accurately represents the experimental data with the scattering from background impurity limiting the low temperature mobility and the scattering from the phonons, both optical and acoustic, limiting the ambient temperature mobility. Only at elevated temperatures, the value predicted by the scattering model deviates from the experimental value due to possible parallel conduction inside the sample, such as the InAlAs buffer layers.

4. Conclusion

In this work an InAs-like LO phonon with an energy of 28.8 meV, a frequency of 232 cm^{-1} is observed in $\text{In}_{0.75}\text{Ga}_{0.25}\text{As}/\text{In}_{0.75}\text{Al}_{0.25}\text{As}$ QWs. The coupling energy of MPR is insensitive to carrier density and substrate materials. The fact that the MPR is observable up to 300 K together with the high mobility, exceeding $1.5 \times 10^4 \text{ cm}^2/\text{V.s}$ at ambient temperature, has demonstrated the high crystalline quality in $\text{In}_{0.75}\text{Ga}_{0.25}\text{As}$ QWs grown by MBE from two substrate materials. A scattering rate model, using the phonon energy measured by MPR to predict the ambient temperature mobility, shows good agreement with the experimental data when a parallel conduction effect in the barriers and buffer layers is small.

5. Acknowledgments

The work was funded by EPSRC Grant No. EP/K004077/1, UK.

References

- [1] International Technology Roadmap for Semiconductors, <http://www.itrs2.net/>
- [2] J. Groenen, R. Carles, G. Landa, C. Guerret-Piecourt, C. Fontaine and M. Gendry, *Phys. Rev. B* 58, 16, 10452 (1998).
- [3] R. J. Nicholas, J.C. Portal, C. Houlbert, P. Perrier and T.P. Pearsall, *Appl. Phys. Lett.* 34, 492 (1979)
- [4] T.P. Pearsall, R. Carles and J.C. Portal, *Appl. Phys. Lett.* 42, 436 (1983)
- [5] J. C. Portal, J. Cisowski, R. J. Nicholas, M. A. Brummell, M. Razeghi and M. A. Poisson, *J. Phys. C: Solid State Phys.*, 16, L573-L578 (1983).
- [6] D. R. Leadley, R. J. Nicholas, L. L. Taylor, S. J. Bass and M. S. Skolnick, *Springer Solid State Sci.* 87, 545 (1988)
- [7] M. A. Brummell, R. J. Nicholas, J. C. Portal, K. Y. Cheng and A. Y. Cho, *J. Phys. C: Solid State Phys.*, 16, L579-L584 (1983).
- [8] R. J. Nicholas, S. Ben Amor, J. C. Portal, D. L. Sivcol and A. Y. Cho, *Semicond. Sci. Technol.* 4, 116-118 (1989)
- [9] D. Ploch, E. M. Sheregii, M. Marchewka, M. Wozny, and G. Tomaka, *Phys. Rev. B* 79, 195434 (2009)
- [10] O. Drachenko, J. Galibert, J. Lotin, J. W. Tomm, M. P. Semtsiv, M. Ziegler, S. Dressler, U. Müller and W. T. Masselink, *Appl. Phys. Lett.* 87, 072104 (2005)
- [11] R. J. Nicholas, *Prog. Quant. Electr.* 10, 1 (1985)
- [12] C. Chen, I. Farrer, S. N. Holmes, F. Sfigakis, M. P. Fletcher, H. E. Beere and D. A. Ritchie, *J. Cryst. Growth*, 425 (2015)
- [13] P. J. Simmonds, H. E. Beere, D. A. Ritchie and S. N. Holmes, *J. Appl. Phys.* 102, 083518 (2007)
- [14] W. Desrat, F. Giazotto, V. Pellegrini, F. Beltram, F. Capotondi, G. Biasiol, L. Sorba and D. K. Maude, *Phys. Rev. B* 69, 245324 (2004)
- [15] T. P. O'Regan, M. V. Fischetti, B. Sore, S. Jin, W. Magnus, and M. Meuris, *J. Appl. Phys.* 108, 103705 (2010)
- [16] <http://www.ioffe.ru/SVA/NSM/Semicond/>
- [17] A. Milekhina, A. Kalagina, A. Vasilenkoa, A. Toropova, N. Surovtsevb and D. R. T. Zahn, *AIP Conference Proceedings*, 1199, 43-44 (2010)
- [18] J. Groenen, G. Landa, R. Carles, P.S. Pizani and M. Gendry, *J. Appl. Phys.*, 82 (2), 803 (1997).

- [19] F. Capotondi, G. Biasiol, I. Vobornik, L. Sorba, F. Giazotto, A. Cavallini, and B. Fraboni, *J. Vac. Sci. Technol. B* 22, 702-706 (2004).
- [20] F. Capotondi, G. Biasiol, D. Ercolani, V. Grillo, E. Carlino, F. Romanato and L. Sorba, *Thin Solid Films*, 484, 400-407 (2005)
- [21] C. Y. Huang, J. J. M. Law, H. Lu, D. Jena, M. J. W. Rodwell and A. C. Gossard, *J. Appl. Phys.* 115, 123711 (2014)
- [22] W. Walukiewicz, H. E. Ruda, J. Lagowski, and H. C. Gatos, *Phys. Rev. B* 30, 4571 (1984)
- [23] A. Gold, *Phys. Rev. B*, 35, 723 (1987)
- [24] P. J. Price, *Ann. Phys.* 133, 217 (1981)